Journal of Alloys and Compounds 504S (2010) S531–S533

Contents lists available at ScienceDirect

Journal of Alloys and Compounds

journal homepage: www.elsevier.com/locate/jallcom

Ab-initio calculations for defect energies in Co_2MnSi and Co_2CrAl

T. Hoshino[a], N. Fujima[b,*], M. Asato[c], H. Tatsuoka[b]

[a] Nanomaterials Section, Graduate School of Science and Technology, Shizuoka University, Hamamatsu 432-8561, Japan
[b] Faculty of Engineering, Shizuoka University, Hamamatsu 432-8561, Japan
[c] Niihama National College of Technology, Niihama 792-8580, Japan

ARTICLE INFO

Article history:
Received 3 July 2009
Received in revised form 12 January 2010
Accepted 10 February 2010
Available online 18 February 2010

Keywords:
Full Heusler alloy
Defect
Ab-initio calculation
KKR

ABSTRACT

The ab-initio band calculations predict that the full-Heusler ferromagnetic alloys at $L2_1$ structure, such as Co_2MnSi and Co_2CrAl, are half-metallic. However, the measured spin polarizations have been usually less than ~60%. The decrease may be attributed to defects of swaps and antisites. We give ab-initio calculations for the formation energies of isolated swaps in Co_2MnSi and Co_2CrAl and isolated antisites in Co_2MnSi, which may be the important factor to determine the defect concentrations. The present calculations predict that two kinds of antisites (Si in Mn-site and Mn in Co-site) in Co_2MnSi and one kind of swap (Cr–Al) in Co_2CrAl, are very likely to be formed because of the small defect energies. Using the calculated results, we clarify the fundamental features of Co_2MnSi and Co_2CrAl with defects and discuss how to understand the discrepancies between the band calculation and experimental results.

© 2010 Elsevier B.V. All rights reserved.

1. Introduction

Ferro-magnetic (FM) full-Heusler alloys at $L2_1$ structure have attracted a great deal of interest during the last century as materials of various high qualities [1,2]. Especially, Co-based alloys, such as Co_2MnSi and Co_2CrAl, were expected as half-metallic(100% spin polarization at the Fermi level) FM alloys with high Curie temperatures. According to the band calculations, the ground states of Co_2MnSi and Co_2CrAl are half-metallic [3–5]. However, the measured spin-polarization have been usually less than ~60% [6] and the measured total magnetic moment of Co_2CrAl is fairy small ($1.55\,\mu_B$) [7], compared with the band calculation result ($3.00\,\mu_B$) [4]. It is also well known experimentally that the atomic structure of Co_2CrAl is B2 (disordering of Cr and Al) [8]. The B2 structure of Co_2CrAl may be considered as the system with the high concentration of Cr–Al swaps in Co_2CrAl. Since the experimental results depend very much on the condition of the fabrication [6], it is easily anticipated that the discrepancies between the band calculation and experimental results may be attributed to defects of swaps and antisites. Thus, the development of the electronic devices of high qualities needs the theoretical study of the electronic states and magnetism of the full-Heusler alloys with and without the defects.

At present, according to our knowledge, there are very few theoretical works for the defect systems, such as the FLAPW calculations by Picozzi et al. [9], using the supercell approximation, and the KKR-CPA calculations by Miura et al. [10], using the spherical potential approximation. Developing the ab-initio calculations based on the full-potential Korringa–Kohn–Rostoker (FPKKR) Green's function method combined with the generalized gradient approximation (GGA) in the density functional theory, we have reproduced the physical quantities of metals with and without defects, such as the atomic structures, the equilibrium lattice parameters, and the bulk moduli of pure elemental metals (Li–Au), and the monovacancy formation energies in them [11].

Using the local-spin-density approximation (LSDA)–FPKKR, Galanakis et al. have already succeeded in elucidating the fundamental features of many half-metallic full-Heusler alloys, namely, the relation for magnetic moments with valence numbers per unit cell, called "the Slater–Pauling rule" [1]. They used the experimental values for the lattice parameters and restricted to the FM states.

Following their works and using the GGA–FPKKR calculations, we have also started to study the magnetism of Co-based, Ni-based, and, Ru-based full Heusler alloys. We have already reproduced the experimental results of these alloys without defects, such as the equilibrium lattice parameters, the ground states of magnetism (FM or anti-FM(AFM)), and the total magnetic moments, and discussed successfully the change of magnetism of Ni_2MnAl (from FM to AFM) [5], which occurs at elevated temperatures.

In the present work, we give the calculated results for the formation energies of isolated swaps in Co_2MnSi and Co_2CrAl, and isolated antisites in Co_2MnSi, and clarify the fundamental features of these alloys with defects, and discuss how to understand the discrepancies between the band calculation and experimental results.

* Corresponding author. Tel.: +81 53 478 1780; fax: +81 53 478 1781.
E-mail address: tsnfuji@ipc.shizuoka.ac.jp (N. Fujima).

0925-8388/$ – see front matter © 2010 Elsevier B.V. All rights reserved.
doi:10.1016/j.jallcom.2010.02.056

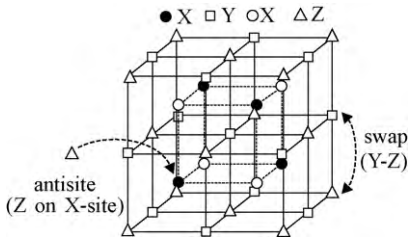

Fig. 1. Atomic structure for $L2_1$ structure of full Heusler X_2YZ alloy and the defects of a swap (Y–Z) and an anitisite (Z on X-site).

2. Method of ab-initio calculations

The calculations for total energies of impurity systems are based on the density functional formalism in the GGA. In order to solve the Kohn–Sham equations we use a multiple scattering theory in the form of the KKR Green's function method for full potentials. The advantage of the Green's function method is that by introducing the host Green's function, the embedding of point defects in an otherwise ideal crystal is described correctly, differently from the usual supercell and cluster calculations [11,12].

It is noted that the potential perturbation due to point defects in metals is very localized in the vicinity of the point defects, because of the screening effect of the host electrons [11]. In the present calculations for the point defect systems, the potential perturbation is taken into account up to the 2nd neighbors around the point defects. The accuracy of the present calculations is discussed in Ref. [11]. It is also noted that the host Green's functions for full-Heulser alloys without defects are obtained very easily by the screened version of KKR calculations in which the short-range structural Green's functions ensure rapid and efficient numerical calculations. The accuracy of the present band calculations for the ideal crystals is discussed in Refs. [5,13–15].

3. Formation energies of swaps and antisites

Fig. 1 shows the atomic structure ($L2_1$) of X_2YZ full-Heusler alloy, and the defects of swaps and antisites. We treat three kinds of isolated swaps (X–Y, Y–Z, Z–X) and six kinds of isolated antisites (Y on X-site, Z on X-site, X on Y-site, Z on Y-site, X on Z-site, Y on Z-site). For example, the Y–Z swap means that the position of Y and Z atoms in the ideal bulk are exchanged, while the anitisite, Z on X-site, means that a X atom is replaced by a Z atom, as shown in Fig. 1. It is noted that the Y–Z swap energy depends on the interatomic distance between Y and Z. It is also noted that the concentrations of elements do not change by the formation of swaps, while they change by the formation of antisites.

The Y–Z swap energy is the total energy change due to the formation of a Y–Z swap. The total energy, $E(\mathrm{Y} \leftrightarrow \mathrm{Z in X_2YZ})$, of the defect system with a Y–Z swap is calculated accurately by the present GGA-FPKKR program for defects. The Y–Z swap energy in X_2YZ is written as follows:

$$\Delta E(\mathrm{Y\text{-}Z\ swap}) = E(\mathrm{Y} \leftrightarrow \mathrm{Z\ in\ X_2YZ}) - E(\mathrm{X_2YZ - bulk}) \quad (1)$$

where $E(\mathrm{X_2YZ - bulk})$ is a total energy of the ideal system without a Y–Z swap.

On the other hand, the calculations for the formation energy due to, for example, an antisite (Z on X-site) in X_2YZ, needs the calculations of total energies of the pure elemental metals (chemical reservoirs) because one Z atom is transferred to a X-site in X_2YZ from a chemical reservoir (elemental Z metal) outside X_2YZ, and one X atom in X_2YZ is transferred to a chemical reservoir (elemental X metal). Thus, the formation energy of the anitisite (Z on X-site) may be written as folows,

$$\Delta E(\mathrm{Z\ on\ X - site}) = E(\mathrm{Z} \rightarrow \mathrm{X\ in\ X_2YZ}) - E(\mathrm{X_2YZ - bulk}) - E(\mathrm{Z - bulk}) + E(\mathrm{X - bulk}) \quad (2)$$

where $E(\mathrm{Z} \rightarrow \mathrm{X\ in\ X_2YZ})$ and $E(\mathrm{X_2YZ - bulk})$ are the total energies with and without an antisite (Z on X-site). $E(\mathrm{Z - bulk})$ and $E(\mathrm{X - bulk})$ are the total energies (per atom) of Z and X metals. All the total energies are calculated by the present ab-initio programs for perfect metals and defect systems, as have been discussed in Section 2.

In the present calculations for antisites in Co_2MnSi, we choose as the stable phases for elements (Co,Mn,Si), the FM hcp Co, the nonmagnetic (NM) hcp Mn, and the diamondlike Si, respectively, which are the calculated ground states among fcc, bcc, hcp, and diamondlike structures [12,16]. The present calculation results for elemental metals agree with the experimental results, except Mn: the observed atomic structure of Mn is αMn. However, it is noted that the energy difference between hcp-NM and α Mn may be as small as a few mRy [17]. Thus, the present results do not change very much on the choice between α Mn and hcp-NM.

Table 1
Three kinds of swap energies (in eV) in Co_2MnSi and Co_2CrAl. The FLAPW results are shown in parentheses. See the text for the interatomic distances of swap pairs.

Co_2MnSi		Co_2CrAl	
Co–Mn	1.06(1.13)	Co-Cr	0.74
Co–Si	3.42	Co–Al	2.41
Mn–Si	1.33(1.38)	Cr–Al	0.31

4. Calculated results for swaps and antisites

We show the calculated results for the formation energies of isolated swaps in Co_2MnSi and Co_2CrAl, and the formation energies of isolated antisites in Co_2MnSi, and clarify the fundamental features, which may be important to understand the discrepancies between the band calculation and experimental results. In the present work, as the first results for swap energies, we treat the swaps of the nearest-neighbor pairs X–Y and X–Z, and the second-neighbor pair Y–Z. The calculated results for swaps in Co_2MnSi and Co_2CrAl are shown in Table 1, while those for antisites in Co_2MnSi in Table 2. The available FLAPW results are also shown in parentheses. The agreement between the calculated results demonstrates the accuracy of both the calculations.

First we discuss the formation energies of isolated swaps in Co_2MnSi and Co_2CrAl, as listed in Table 1. It is noted that the swap energies in Co_2CrAl are small, compared with the results of Co_2MnSi. Especially, the (Cr–Al) swap energy is very small (0.31 eV). The swap (Co–Cr) energy (0.74 eV) is also small, compared with the values of other swaps. This means that the exchange of Cr and Al is very likely to be formed in Co_2CrAl. This result agrees with the experimental results of the disordering (B2 structure) of Cr and Al in Co_2CrAl [8], although the quantitative discussions need the molecular dynamic calculations with the accurate model potential [18], for more complex systems with different kinds of swaps and antisites.

Table 2
Six kinds of antisite energies (in eV) in Co_2MnSi. The FLAPW results are shown in parentheses.

Mn on Co-site	0.32(0.33)
Si on Co-site	2.20
Co on Mn-site	0.79(0.80)
Si on Mn-site	0.27
Co on Si-sie	2.22
Mn on Si-site	1.35

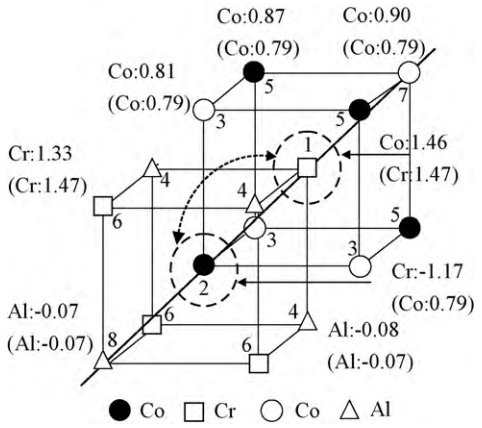

Fig. 2. Distribution of magnetic moments around a Co–Cr swap in Co_2CrAl, with the c_{3v} symmetry around a Co–Cr swap. The magnetic moments in an ideal Co_2CrAl alloy are shown in parentheses. It is noted that the three Cr–Cr pairs of anti-ferromagnetic coupling are created as a result of the formation of a Co–Cr swap. See the text for details.

It is also known that the measured value of total magnetic moment (MM) of Co_2CrAl is very small ($1.55\,\mu_B$), compared with the band calculation result($3.00\,\mu_B$). This discrepancy may be understood by considering the creation of the 1st-neighbor Cr–Cr pairs, for example, which occurs as a result of the formation of Co–Cr swaps [10], as follows.

Fig. 2 shows the calculated results for the MM distribution around an isolated Co–Cr swap. We found that the change (90%) of the total MMs with respect to the ideal value is due to the change of MMs in the sites shown in Fig. 2, being the two sites in a Co–Cr swap and the nearest-neighboring sites around a Co–Cr swap. According to the present calculations, the ground state of the magnetism of the 1st-neighbor Cr–Cr coupling is AFM and the total MM decrease is as large as $2.22\,\mu_B$ per Co–Cr swap. Thus, the measured decrease ($1.45 = 3 - 1.55\,\mu_B$) of the total MM of Co_2CrAl may be understood by considering the appropriate concentration of Co–Cr swaps.

Now we discuss the calculated results for isolated antisites in Co_2MnSi, listed in Table 2. We found that two kinds of antisites, such as Si on Mn-site and Mn on Co-site, are very likely to be formed because of the small energies (0.27 eV and 0.32 eV). We estimate the equilibrium concentration c_{defect} of the defects at temperature T, by using a simple Boltzmann-like distribution,

$$c_{defect} = \exp\left(-\frac{\Delta E}{k_B T}\right). \quad (3)$$

In particular, considering a temperature $T = 1523\,K$, suitable for a triarc Czochralski growth of bulk Co_2MnSi [6], the equilibrium concentrations of two defects (Si on Mn-site and Mn on Co-site) are as large as 13% and 8%, respectively. The result (8%) for Mn in Co-site agrees with 5–7%, which was obtained by the analysis of the neutron diffraction measurements [6]. For Si on Mn-site, there are no information on its concentration, although the formation of Si on Mn-site was confirmed by the analysis of the measured X-ray radiation diffraction patterns [19]. Thus, the comparison of the present result with the experimental result is a future problem.

Before closing this section, we discuss one possibility to explain the decrease of the spin polarization at the Fermi level. According to the present calculations, the changes of MMs are very localized around the antisites and the change of total MMs per antisite are $-2.25\,\mu_B$ and $-3.62\,\mu_B$, respectively, for Mn on Co-site and Si on Mn-site. It is obvious that the large deviation from the integer value of the total MM means that the gap states emerge in the minority band and are located at the Fermi level. Thus, we may expect that the decrease of the spin polarization may be understood by considering the antisite (Si on Mn-site) in Co_2MnSi.

5. Summary

We calculated the formation energies of isolated swaps and isolated antisites in Co_2MnSi and Co_2CrAl and showed that the defects, such as one kind of swap (Cr–Al) in Co_2CrAl and two-kinds of antisites (Si on Mn-site, Mn on Co-site) in Co_2MnSi, are likely to be formed because of the small defect energies. We also clarified the fundamental features of these alloys with the defects, and showed how to understand the discrepancies between the band calculation and experimental results, such as the decrease of the spin polarizations in Co_2MnSi , and the disordering of Cr–Al and the decrease of total MM in Co_2CrAl.

One of the authors (T. Hoshino) thanks Prof. K. Inomata and Prof. Y. Sakuraba for useful discussions. This work was supported by Grand-in-Aid for Scientific Research from the Ministry of Education, Culture, Sports, Science and Technology, Japan (20560614).

References

[1] P.H. Galanakis, Dederichs (Eds.), Half-metallic Alloys: Fundamental and Applications (Lecture Notes in Physics, vol. 676), Springer, Berlin, 2005.
[2] P.J. Webster, K.R.A. Ziebeck, H.R.J. Wijn, in: Heusler Alloys and Compounds of d-Elements with Main Group Elements (Landolt–Bornstein-Group III Condensed Matter, Part 2, vol.19c), Springer, Berlin, 1988.
[3] S. Fujii, S. Sugimura, S. Ishida, S. Asano, J. Phys.: Condens. Matter. 2 (1990) 8583.
[4] H.C. Kandpal, G.H. Fecher, G. Felser, J. Phys. D: Apply. Phys. 40 (2007) 1507–1523.
[5] M. Asato, M. Ohkubo, T. Hoshino, F. Nakamura, N. Fujima, H. Tatuoka, Mater. Trans. 49 (2008) 1760–1767.
[6] M.P. Raphael, B. Ravel, Q. Huang, M.A. Willard, S.F. Cheng, B.N. Das, R.M. Stroud, K.M. Bussmann, J.H. Claaasen, V.G. Harris, Phys. Rev. B66 (2002) 104429.
[7] K.H.J. Buschow, P.G. van Engen, J. Mag. Mag. Matter. 25 (1981) 90–96.
[8] S. Okamura, R. Goto, S. Sugimoto, N. Tezuka, K. Inomata, J. Appl. Phys. 96 (2004) 6561–6564.
[9] S. Picozzi, A. Continenza, A.J. Freenman, Phys. Rev. B66 (2002) 094421.
[10] Y. Miura, K. Nagao, M. Shirai, P. Shirai, Phys. Rev. B69 (2004) 144413.
[11] T. Hoshino, T. Mizuno, M. Asato, H. Fukuyama, Mater. Trans. 42 (2001) 2206.
[12] T. Hoshino, M. Asato, R. Zeller, P.H. Dederichs, Phys. Rev. B70 (2004) 094118.
[13] R. Zeller, Phys. Rev. B 55 (1997) 9400.
[14] R. Zeller, M. Asato, T. Hoshino, J. Zabloudil, P. Weinberger, P.H. Dederichs, Philos. Mag. B 78 (1998) 417.
[15] M. Asato, A. Settles, T. Hoshino, T. Asada, S. Blugel, R. Zeller, P.H. Dederichs, Phys. Rev. B60 (1999) 5202–5210.
[16] T. Hoshino, M. Asato, N. Fujima, Intermetallics 14 (2006) 908–912.
[17] M.J. Mehl, D.A. Papaconstantopoulos, Phys. Rev. B54 (1996) 4519.
[18] M. Asato, R. Tamura, N. Fujima, T. Hoshino, Mater. Sci. Forum 561–565 (2007) 1259–1262.
[19] Y. Sakuraba, M. Hattori, M. Onogane, H. Kubota, Y. Ando, A. Sakuma, N.D. Telling, P. Keatley, G. van der Laan, E. Arenholz, R.J. Hicken, T. Miyazaki, J. Magn. Soc. Jpn. 31 (2007) 338–343.